

# Calculating reionization: 3D radiative transfer in an inhomogeneous medium

Alexei O. Razoumov<sup>?</sup> and Douglas Scott<sup>Y</sup>

Department of Physics & Astronomy, University of British Columbia, Vancouver B.C. V6R 1Z4, Canada

original form Oct. 1998

## ABSTRACT

A numerical scheme is proposed for the solution of the three-dimensional radiative transfer equation with variable optical depth. We show that time-dependent ray tracing is an attractive choice for simulations of astrophysical ionization fronts, particularly when one is interested in covering a wide range of optical depths within a 3D clumpy medium. Our approach combines the explicit advection of radiation variables with the implicit solution of local rate equations given the radiation field at each point. Our scheme is well suited to the solution of problems for which line transfer is not important, and could, in principle, be extended to those situations also. This scheme allows us to calculate the propagation of supersonic ionization fronts into an inhomogeneous medium. The approach can be easily implemented on a single workstation and also should be fully parallelizable.

**Key words:** radiative transfer { methods: numerical { cosmology: theory { intergalactic medium

## 1 INTRODUCTION

Understanding the effect of the radiation field on the thermal state of interstellar and intergalactic gas is important for many areas of astrophysics, and in particular for star and galaxy formation. Of special interest for cosmological structure formation are the epoch of reionization of the Universe (Gnedin & Ostriker 1997), the effects of self-shielding on the formation of disk and dwarf galaxies (Navarro & Steinmetz 1997, Kepner et al. 1997) and the absorption properties of Ly clouds (Meiksin 1994). While our knowledge of the physics of large-scale structure and galaxy formation has benefited significantly from numerical N-body and gas-dynamical models, there is very little that has been done to include radiative transfer (RT) into these simulations. Challenges seem to abound, not least of all, the fact that the intensity of radiation in general is a function of seven independent variables (three spatial coordinates, two angles, frequency and time). While for many applications it has been possible to reduce the dimensionality (e.g. to build realistic stellar atmosphere models), the clumpy state of the interstellar or intergalactic medium does not provide any spatial symmetries. Moreover, coupled equations of radiation hydrodynamics (RHD) have very complicated structure, and are often of mixed advection-diffusion type which makes it

very difficult to solve them numerically. Besides that, the radiation field in optically thin regions usually evolves at the speed of light, yielding an enormous gap of many orders of magnitude between the characteristic time-scales for a system.

One way to avoid the latter problem is to solve all equations on the fluid-flow time-scale. While there are arguments which seem to preserve causality in such an approach (Mihalas & Mihalas 1984), even then the numerical solution is an incredibly difficult challenge (Stone et al. 1992). On the other hand, several astrophysical problems allow one to follow the system of interest on a radiation propagation time-scale, without in posing a prohibitively large number of time steps. In the context of cosmological RT, we would like to resolve the characteristic distance between the sources of reionization. Cold dark matter (CDM) cosmologies predict the collapse of the first baryonic objects as early as  $z = 30 - 50$ , with the typical Jeans mass of order  $10^5 M_{\odot}$  (see Haiman & Loeb 1997, and references therein). The corresponding comoving scale of fragmenting clouds is  $\sim 7$  kpc. If stellar sources reside in primordial globular clusters of this mass, then for  $\delta_b = 0.05$  the average separation between these objects is  $\sim 20$  kpc (comoving). For explicit schemes the Courant condition imposes a time-step

$$t_{\text{step}} \approx t_R = \frac{x}{c(1+z)} \approx \frac{10^5}{1+z} h^{-1} \text{ yrs} \quad (1)$$

The evolution from  $z = 20$  to  $z = 3$  takes  $\sim 7.5 \times 10^8 h^{-1} \text{ yrs}$

<sup>?</sup> e-mail: razoumov@astro.ubc.ca

<sup>Y</sup> e-mail: dscott@astro.ubc.ca

(assuming density parameter  $\Omega_0 = 1$ , and defining the Hubble constant to be  $H_0 = 100 \text{ h km s}^{-1} \text{ Mpc}^{-1}$ ). Substituting  $z = 3$  and  $z = 20$  into eq. (1) yields the total number of time-steps in the range 20;000–150;000 over the entire course of evolution. In other words, to resolve reionization by  $10^5 \text{ M}$  stellar clusters, we need to compute a few tens of thousands of time-steps on average. For  $10^8 \text{ M}$  clusters the number of steps required will be ten times smaller. A  $100^3$  grid will result in computational boxes of several  $\text{Mpc}$  on a side. A full cosmological radiative transfer simulation with boxes at least this big and for all the required time-steps has hardly been feasible in the past.

This is not the only challenge we face. Since any two points can affect each other via the radiation field, even for a monochromatic problem, we must describe the propagation of the radiation field anisotropies in the full 6-dimensional space. Standard steady-state RT solvers, which have been widely used in stellar atmosphere models, are not efficient in this case. Non-local thermodynamic equilibrium (NLTE) steady-state radiative transport relies on obtaining the numerical solution via an iterative process for the whole computational region at once, and is usually effective only for very simplified geometries. Any refinement of the discretization grid and/or increase in the number of atomic rate equations to compute NLTE effects will necessarily result in an exponential increase in the number of iterations required to achieve the same accuracy. On the other hand, the 3D solution of the steady-state transfer equation in the absence of any spatial symmetries can often be obtained with Monte Carlo methods (Park & Hong 1998). However, these methods demonstrate very slow convergence at higher resolutions and are hardly applicable if one is interested in following a time-dependent system.

The change in the degree of ionization in a low-density environment occurs on a radiation propagation time-scale  $t_R$ . To track ionization fronts (I-fronts) in this regime, it is best to apply a high-resolution shock-capturing scheme similar to those originally developed in fluid dynamics. One possible approach is the direct numerical solution of the monochromatic photon Boltzmann equation in the 5-dimensional phase space (Razoumov, in preparation). To allow for a trade-off between calculational speed (plus memory usage) and accuracy, a more conventional approach is to truncate the system of angle-averaged radiation moment equations at a fixed moment and to use some closure scheme to reconstruct the angle dependence of the intensity at each point in 3D space. The method of variable Eddington factors first introduced by Auer & Mihalas (1970) has been shown to produce very accurate closure for time-dependent problems in both 2D (Stone et al. 1992) and 3D (Umehura et al. 1998). However, to the best of our knowledge, all schemes employed so far for calculating the time-dependent variable Eddington factor were based on a steady-state reconstruction of the radiation field through all of the computational region at once, given the thermal state of material and level populations at each point. Since advection (or spatial transport) of moments is still followed on the time-scale of typical changes in the ionizational balance of the system, this approximation certainly provides physically valid results, assuming that the reconstruction is being performed often enough. However, the steady-state closure relies on the iterative solution of a large system of non-linear equations,

which becomes an exceedingly difficult problem, from the computational point of view, as one moves to higher spatial and angular resolution and to the inclusion of more complicated microphysics.

The goal of the present paper is to demonstrate that in the cosmological context it is possible and practical to solve the whole RT problem on a radiation propagation time-scale  $t_R$  (as opposed to the fluid-flow time-scale) and we present a simple technique which gives an accurate solution for the angle-dependent intensity in three spatial dimensions. The scheme can track discontinuities accurately in 3D and is stable up to the Courant number of unity. Since all advection of radiation variables is being done at  $t_R$ , the scheme is well tailored to the numerical study of the propagation of I-fronts into a non-homogeneous medium (Razoumov, in preparation).

This paper is organized as follows. In Section 2 we briefly review the state of numerical RT in the study of reionization. We then concentrate on methods for 5D numerical advection. In Section 3 we describe our numerical algorithm and we present the results of numerical tests in Section 4. Finally, in Section 5 we discuss the next steps towards a realistic 3D RT simulation.

## 2 FORMULATION OF THE PROBLEM

It is believed that light from the first baryonic objects at  $z > 6$  led to a phase-like transition in the ionizational state of the Universe. This process of reionization significantly affected the subsequent evolution of structure formation (Couchman & Rees 1986). In detail reionization did not happen at a single epoch, with details of ‘pre-heating’, percolation, helium ionization and other physical processes having been studied in great detail over the last decade (some recent contributions include Madau et al. 1997, Haiman & Loeb 1997, Gnedin & Ostriker 1997, Shapiro et al. 1998, Tajiri & Umehura 1998).

It now seems clear that the full solution of the problem requires a detailed treatment of the effects of RT. To complicate matters, by the time of the first star formation, the small-scale density inhomogeneities have entered the non-linear regime (Gnedin & Ostriker 1997), and the medium was filled with clumpy structures. The success of cosmological N-body and hydrodynamical models in quantifying the growth of these objects (e.g., Zhang et al. 1998) suggests that the next step will be to include the effects of global energy exchange by radiation. Indeed, there is a need for time-dependent 3D RT models as numerical tools for understanding the effect of inhomogeneities in the dynamical evolution of the interstellar/intergalactic medium. For instance, the ability of gas to cool down and form structures depends crucially on the ionizational state of a whole array of different chemical elements, which in turn directly depends on the local energy density of the radiation field.

The hydrogen component of the Universe is most likely ionized by photons just above the Lyman limit, because (1) the cross-section of photoionization drops as  $\nu^{-3}$  at higher frequencies, and (2) the medium will be dominated by softer photons, even in the case of quasar reionization (when ionizing photons come mostly from diffuse H II regions). There-

fore, we argue that monochromatic transfer will be a fairly good approximation in our models.

Several research groups have made significant progress in simulating 3D inhomogeneous reionization. Recently, Umemura et al. (1998) calculated reionization from  $z = 9$  to  $z = 4$ , solving the 3D steady-state RT equation along with the time-dependent ionization rate equations for hydrogen and helium. The radiation field was integrated along spatial dimensions using the method of short characteristics (Stone et al. 1992). The steady-state solution implies the assumption that the radiation field adjusts instantaneously to any changes in the ionization profile. One drawback of this approach, however, is in low-density voids where there are probably enough Lyman photons to ionize every hydrogen atom, so that the velocity of I-fronts is simply equal to the speed of light. Then the rate equations still have to be solved on the radiation propagation timescale. Besides, implicit techniques in the presence of inhomogeneities will become exponentially complicated, if we want to solve time-dependent rate equations for multiple chemical species.

If reionization by quasars alone is ruled out (Madau 1998, however see Hamann & Loeb 1998), then I-fronts will be caused by Lyman photons from low-luminosity stellar sources at high redshifts. In this case the pressure gradient across the ionization zone is more likely to become important before the front is slowed down by the finite recombination time. Norman et al. (1998) outline a scheme for incorporating inhomogeneous reionization with hydrodynamical effects which arise when the speed of I-fronts drops close to the local sound speed. In their method the default time-step is dictated by the speed of the atomic processes, and the radiation field is reconstructed through an elliptic solver (a quasi-static approximation).

In the present paper we ignore hydrodynamical effects, concentrating on an efficient method to track supersonic I-fronts. Our approach is to solve the time-dependent RT coupled with an implicit local solver for the rate equations. This method gives the correct speed of front propagation and it also quickly converges to a steady-state solution for equilibrium systems. However, we should note that until a detailed comparison is made between explicit advection (at the speed of light) and the implicit reconstruction (through an elliptic solver), it is difficult to judge which approach works best in simulating inhomogeneous reionization in detail.

Although radiation propagates with the speed of light and the intensity of radiation depends on five spatial variables, plus frequency and time, the RT equation is inherently simpler than the equations of compressible hydrodynamics, since its advection part is strictly linear. Non-linearities are usually introduced when we are trying to reduce the dimensionality of the problem. Much of the difficulty, thus, comes from inability to get decent numerical resolution in the 5D (or 6D with frequency) space with present-day computers.

In the current work we have attempted to develop an efficient method to describe the anisotropies in the monochromatic radiation field propagating through an inhomogeneous medium, which we now describe.

### 3.1 Time-dependent ray tracing

The RT equation (without cosmological terms) reads

$$\frac{1}{c} \frac{\partial I}{\partial t} + n_r I = \kappa I; \quad (2)$$

where  $I$  is the intensity of radiation in direction  $n$  and  $\kappa$  and  $\epsilon$  are the local emissivity and opacity. In a static medium integration over all directions and frequencies inside some range  $\nu_1$  to  $\nu_2$ , with corresponding weights, yields the system of moment equations, the first two of which are

$$\frac{\partial E}{\partial t} = \kappa_r F + 4 \kappa_s S - c E \epsilon; \quad (3)$$

$$\text{and } \frac{1}{c^2} \frac{\partial F}{\partial t} = \kappa_r P - \frac{1}{c} F \epsilon; \quad (4)$$

Here we have introduced the frequency-averaged opacities

$$\kappa_r = \frac{F}{F^2} \int \kappa_r(\nu) d\nu; \quad (5)$$

$$\kappa_s = \frac{1}{S} \int \kappa_s(\nu) d\nu; \quad (6)$$

$$\kappa_e = \frac{1}{E} \int \kappa_e(\nu) d\nu; \quad (7)$$

Here  $E$ ,  $F$  and  $P$  are the first three moments (zero, first and second rank tensors, respectively) of the specific intensity  $I$ .

The basic idea of our technique is to use an upwind monotonic scheme to propagate 1D wavefronts along a large number of rays in 3D at the speed of light. Following Stone & Mihalas (1992), we apply an operator split explicit-implicit scheme, in which advection of radiation variables is treated explicitly and the atomic and molecular rate equations are solved implicitly and separately at each point. The whole computational volume is covered uniformly with rays, which makes this scheme geometrically similar to the method of long characteristics' discussed in Stone, Mihalas & Norman (1992). Since the advection part on the left-hand side of eq. (2) is strictly linear, the simplest way to propagate intensities is just to shift wavefronts by one grid zone at each time step accounting for sources and sinks of radiation. Alternatively, one could use the third-order-accurate piecewise parabolic advection (PPA) of Stone & Mihalas (1992). In either case we can track sharp discontinuities in 1D with very little numerical diffusion, and, therefore, our approach is well suited to the calculation of I-fronts.

At each new time step, we project 1D intensities onto a 3D grid to reconstruct the mean energy density at each point. This is the most demanding operation from the computational point of view, since at each of our  $N^3$  points we have to deal with the angular dependence of the radiation field. When this update is done, we solve the matter-radiation interaction equations implicitly to compute the local level populations. This gives us the 3D distributions of emissivity and opacity which are then mapped back to the rays and used in the advection scheme at the next time-step. This simple scheme which we will refer to as time-dependent ray tracing can be used as a stand-alone solver, or as a closure scheme for the system of moment equations through the use of variable Eddington factors (as in Stone et al. 1992).

In the absence of any sinks and sources of radiation, the intensity is conserved exactly along each ray. Since the num -

ber of rays does not vary with time, our method guarantees exact conservation of the radiation energy in 3D.

One advantage of the use of radiation moments is that the advection mechanism is essentially reduced to 3D, and it is relatively straightforward to implement the multidimensional conservation scheme for the linear advection part of the moment equations (3) and (4). Then one could use a much denser spatial grid for the solution of the moment equations, and a relatively coarse grid for the angular reconstruction of the intensity of radiation via ray tracing. In practice, however, we have found that the mismatch between the spatial resolutions of the moment solver and of the ray tracing usually leads to numerical instabilities. In what follows, we consider ray tracing only as a stand-alone solver, and we will describe the merging of the moment solver and the ray tracing elsewhere (Razoumov, in preparation).

The most obvious drawback of time-dependent ray tracing is the need to use a large number of rays to obtain an accurate description of the radiation field. However, efficient placing of the rays can significantly reduce the number of operations. Ultimately we are interested in getting a solution for the mean radiation energy density and material properties on a 3D rectangular grid. Instead of shooting rays through each grid node in 3D, we choose to cover the whole computational volume with a separate grid of rays which is uniform both in space and in angular directions. To reduce the Poisson error associated with a Monte-Carlo integration, we use high-order interpolation techniques to exchange data between the two grids. Since the rays do not pass exactly through 3D grid points, we use four rays in any given direction to compute the angular-dependent intensity. At each point on our 3D rectangular mesh we assume a piecewise linear dependence of the intensity  $I$  on two angles, and we then integrate the intensity over 4 with appropriate weights to get scalar quantities at each point. The quadrature terms for the integration are modified to allow for the non-orthogonal angular grid and are calculated once, at the beginning of the simulation.

Another (perhaps, a better) way of coupling angular and spatial variations of the intensity may be an extension of the Spherical Harmonics Discrete Ordinate Method (Evans 1998). For steady-state transfer problems, instead of storing the radiation field, this method stores the source function as a spherical harmonic series at each point. Although the direct implementation of this technique for time-dependent problems is probably not realistic, due to the lookback time (i.e. the finite speed of light propagation), the spherical harmonic representation of the radiation field might require less storage and might result in smoother angular dependence as compared with a pure ray tracing approach.

### 3.2 Local chemistry equations

Abel et al. (1997) presented a detailed method for computing non-equilibrium primordial chemistry. Since in our calculation all advection of radiation variables is performed explicitly, we can solve NLTE rate equations separately at each point. This makes it very easy to implement an implicit solver for all atomic and molecular processes.

Following the primordial chemistry recipe of Abel et al. (1997) and Anninos et al. (1997), rate equations for nine species ( $H$ ,  $H^+$ ,  $H_2$ ,  $H_2^+$ ,  $He$ ,  $He^+$ ,  $He^{++}$  and  $e^-$ ) have

been included into the model. The resulting six equations can be stored in the compact form:

$$\frac{\partial n_i}{\partial t} = \sum_j \sum_k X_{jk} n_j n_k + \sum_j X_{ji} n_j; \quad (8)$$

with indices corresponding to individual species. To demonstrate the capabilities of explicit advection, we have here reduced this set of equations to just photoionization and radiative recombination in a pure hydrogen medium. The time evolution of the degree of ionization is given simply by

$$\frac{dx}{dt} = (1-x)g_H I_E - x^2 n_H; \quad (9)$$

with emissivity and opacity

$$= \frac{h\nu}{4} (xn_H)^2 \gamma_1; \quad (10)$$

$$= (1-x)n_H h\nu \gamma_H I = C; \quad (11)$$

The full recombination coefficient

$$= \gamma_1 + \gamma_B \quad (12)$$

is the sum of recombination coefficients to the ground state ( $\gamma_1$ ) and to all levels above the ground state ( $\gamma_B$ , the 'base B' recombination coefficient),  $\gamma_1$  is the frequency just above the Lyman limit, and we assume that recombinations in Lyman lines occur on a short timescale compared to  $(xn_H \gamma_B)^{-1}$ . This simple notation ensures radiation energy conservation in eq. (2) for pure scattering of Lyman continuum photons (i.e., when  $\gamma_B = 0$ ).

## 4 TESTS

For all of our test runs, except the study of the shadow behind a neutral clump in Sec. (4.3), we set up a numerical grid with dimensions  $64^3 \times 10^2$ . The angular resolution  $N_{dir}^2 = 10^2$  was chosen to match the equivalent resolution of  $64^5$  data points for 5D advection. There are  $N_{dir}^2$  rays passing in the immediate neighbourhood ( $1=64^3$ th of the total computational volume) of each 3D grid cell, each ray containing  $N_p = 2 \times 3 \times 64$  grid nodes. Thus, in 5D we obtain the equivalent resolution of  $N_p = 64^3 \times N_{dir}^2 = 1.1 \times 10^9 \times 64^5$  data points.

### 4.1 An isolated Stromgren sphere in the presence of a density gradient

The simplest test possible is that of a single, isolated Stromgren sphere expanding around a point source of ionizing radiation. In the context of quasar reionization for a homogeneous medium the exact solution was given by Shapiro (1986). We consider this test so easy to pass that the results would prove uninformative. Instead, we put a point source of radiation into a density gradient along one of the principal axes of the cube. In the absence of diffuse radiation from H II regions ( $\gamma_1 = 0$ ) the only ionizing photons come directly from the source in the centre, in which case the shape of the ionized bubble would be a simple superposition of Stromgren spheres with radii  $R_S(\theta)$  varying with the azimuthal angle  $\theta$  and given by the classical solution (Spitzer 1968)

$$S_0 = 4 \int_0^{R_S} r^2 n_H^2(r) dr; \quad (13)$$

where  $S_0$  is the photon production rate of the central source. For an exponential density gradient along the y-axis

$$\log n_H = \log n_{H,1} + \frac{r \cos \theta + y_0}{y} \log \frac{n_{H,2}}{n_{H,1}} \quad (14)$$

( $n_{H,1}$ ,  $n_{H,2}$  being the hydrogen densities on the opposite faces of the cube), the equilibrium Stromgren radius  $R_S(\theta)$  is given by a simple equation

$$S_0 = \frac{4}{b^3} e^{a + bR_S(\theta)} (b^2 R_S^2(\theta) - 2bR_S(\theta) + 2) 2e^a; \quad (15)$$

where

$$a = 2 \ln n_{H,1} + \frac{y_0}{y} \ln \frac{n_{H,2}}{n_{H,1}} \quad \text{and}$$

$$b = \frac{2 \cos \theta}{y} \ln \frac{n_{H,2}}{n_{H,1}};$$

In Fig. 4.1 we plot a time sequence of models with ionization by a central source without scattering of Lyman photons ( $\tau = 0$ ) and with complete scattering ( $\tau_B = 0$ ). The numerical solution without scattering appears to be very close to the exact one. The sharp transition layer between the ionized and the neutral regions in the low optical depth regime indicates that, indeed, the scheme introduces very little numerical diffusion even when extended to 3D. There is slight asymmetry between the left- and the right-hand sides of the I-front, which is left in the algorithm intentionally to demonstrate the effect of the finite angular resolution (Fig. 4.1).

Ideally, one would like to place more rays going through individual point sources of radiation. However, in a dynamically changing environment the number and positions of sources will vary with time. There is nothing in our scheme that precludes allocation of new rays as new sources appear in the volume. As long as all rays employed so far are kept in the model, we can guarantee the exact conservation of energy. Methods could probably be developed to remove rays when ionizing sources shut off. Another and, in our mind, more promising way to deal with evolving point sources is to use the 5D solution of the monochromatic photon Boltzmann equation separately for those sources, and the ray tracing model outlined in this paper for the background radiation.

#### 4.2 Ionization in the presence of a UV background

The uniform coverage of the whole volume with rays implies that extended sources of radiation will be represented statistically much better than point sources. A simple test mimicking the evolution of dense clouds in the presence of ionizing radiation is to enclose the computational region in an isotropic bath of photons. The simplest way to accomplish this is just to set up a uniform, isotropically glowing boundary at the edges of the cube at  $t = 0$ . An effective demonstration of time-dependent ray tracing would be its ability to deal with any distribution of state variables within the simulation volume. For this test, we set up a density condensation shaped as the acronym for 'radiation hydrodynamics'

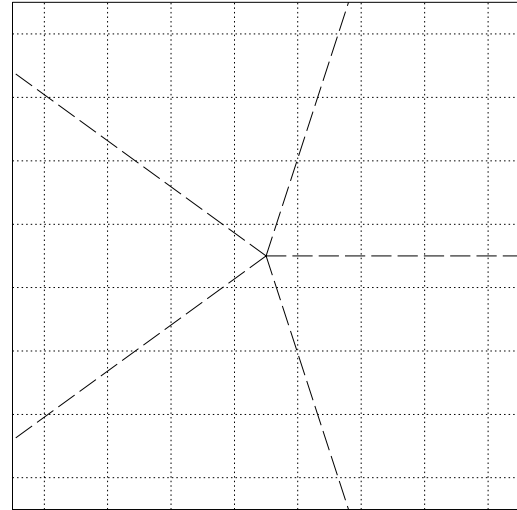


Figure 2. In order to cover the whole computational volume with rays uniformly and isotropically, we set the number of rays inside a latitudinal angle interval  $[\theta; \theta + d\theta]$  proportional to  $\cos \theta$ . An odd number of rays will necessarily introduce slight left-right asymmetry for interpolation between the 3D rectangular grid and the radial grid for any non-central cross-section through the volume. In this figure we show a 2D schematic representation of the two grids employed in our method. To simplify the plot, the source of radiation is assumed to be sitting in the centre, and only radial rays are drawn here. Due to the finite angular resolution, interpolation between the 3D mesh and the rays is not symmetric with respect to the centre. This shows up in the asymmetry between the left- and the right-hand sides of the ionization contours in Fig. 4.1.

(RHD), with a density  $10^{12}$  times that of the ambient homogeneous medium. Fig. 4.2 shows the result of this run. Most of the low-density environment is ionized on the radiation propagation timescale. It takes much longer for ionizing photons to penetrate into the dense regions. Whether these regions can be ionized on a timescale of interest, depends on the ratio of the recombination timescale to the flux of background radiation. During partial ionization one can easily notice shadows in between the clouds. One can also see ionization 'eating in' to the neutral zone, e.g. in the disappearance of the serifs on the letters at late times. Note that the width of the ionization fronts does not usually exceed one grid zone (Fig. 4.2).

#### 4.3 Diffuse radiation from H II regions: shadows behind neutral clouds

Part of the ionizing radiation at high redshifts comes in the form of hydrogen Lyman continuum photons from recombinations in diffuse ionized regions. The following test simulating the formation of shadow regions behind dense clouds at the resolution  $32^3 \times 10^2$  was adapted from Canto, Steen & Shapiro (1998). A neutral clump of radius  $R_c$  is being illuminated by a parallel flux  $F$  of stellar ionizing photons from

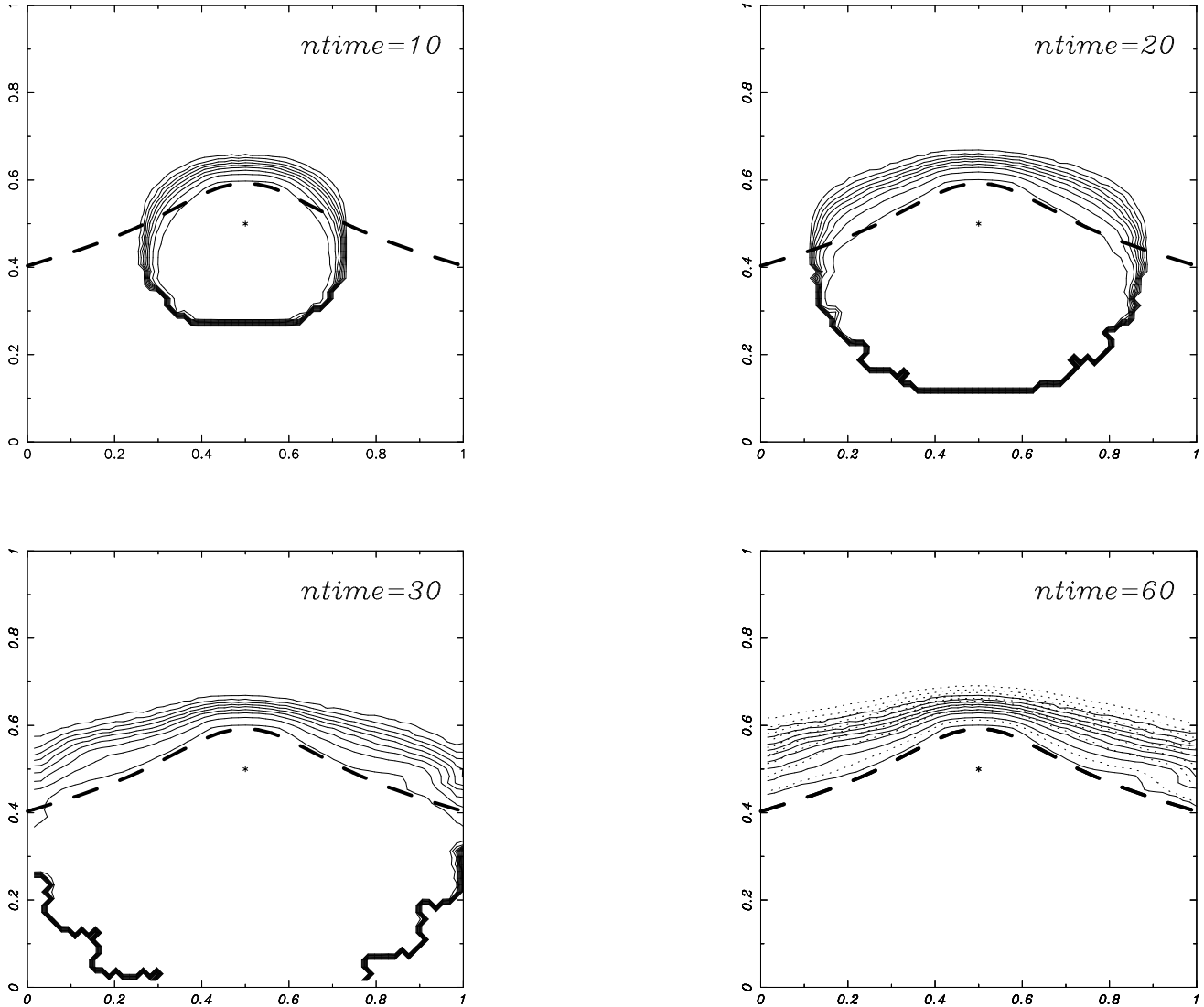


Figure 1. The cross-section of the numerical 3D ionization front going through the source of ionization is shown for four output times. The density of the gas follows an exponential gradient (Eq.14) increasing by a factor of  $10^8$  from the lower to the upper side of the cube. The dashed line gives the simplified analytic solution (Eq.15) for no scattering. Note the sharpness of the transition layer between the neutral and fully ionized regions in the low-optical depth regime. The ionizing source is marked by the asterisk. The solid contour lines correspond to a model with no scattering ( $\tau_B = 0$ ), while the dotted lines on the last snapshot show a model with complete scattering ( $\tau_B = \infty$ ). The nine contour levels correspond to ionization fractions of  $x = 0.1; 0.2; \dots; 0.9$ .

one side. A shadow behind the clump is being photoionized by secondary recombination photons from the surrounding  $H\ II$  region (Fig. 4.3). Neglecting hydrodynamic effects, the width  $R_I$  of the shadow region can be estimated using a simple two-stream approximation (Canto et al. 1998):

$$\tau^2 = \frac{2}{1 + r_i^2 (2 \ln r_i - 1)}; \quad \text{where } r_i = \frac{R_I}{R_c}; \quad (16)$$

and the dimensionless parameter  $\tau$  is defined as

$$\frac{4R_c D_H^2}{F} \frac{\tau^2}{1}; \quad (17)$$

For  $\tau^2 \ll 2$ , recombination Lyman continuum photons from the illuminated region will eventually photoionize the shadow completely. For  $\tau^2 > 2$ , radiative losses through low-

energy cascade recombination photons will stop the I-front, forming a neutral cylinder behind the dense clump. Strictly speaking, equations (16)-(17) are valid only for a shadow completely photoionized by secondary photons, and should be viewed as an approximation to I-fronts driven by secondary photons. In Fig. 4.3 we plot the radius  $R_I$  of the shadow neutral region as a function of  $\tau$  in our 3D numerical models. Due to the finite accuracy of our simulations we take the width of the neutral core of the shadow at a non-zero level  $x = 0.1$ , instead of the exact outer boundary of the neutral region at  $x = 0$ . This approximation essentially shifts the position of the curve in Fig. 4.3 along the  $\tau$ -axis, giving slightly different values for the flux of scattered photons. For convenience, we also plot a sequence of solutions

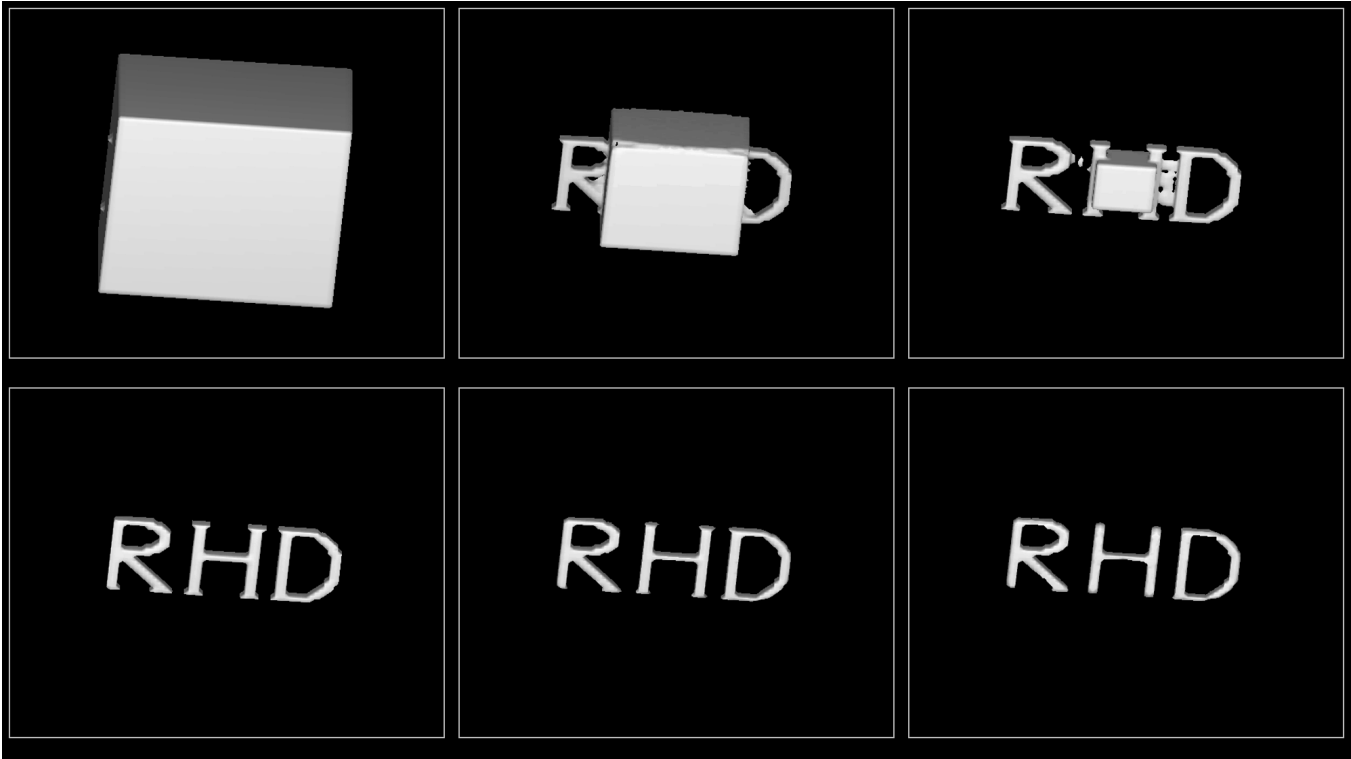


Figure 3. The isosurface of ionization level  $x = 0.5$  is plotted at six time intervals for the model with an ionizing background coming from outside of the cube. The density contrast between the ambient medium and the high-density acronym ‘RHD’ (radiation hydrodynamics) is  $10^{12}$ . This simulation demonstrates 5D advection on the radiation propagation time-scale. The numerical resolution is  $64^5$ . Besides photoionization we include recombination on a much shorter time scale. The effects of shielding are clearly visible during partial ionization.

from equations (16)–(17) for different fluxes of scattered radiation (which are, in turn, proportional to  $F$ ). We find fairly close correspondence between the shape of the curve in our models and the analytic solution, within the limits of the simplifying assumptions made for the analytic solution.

#### 4.4 Diffuse radiation from H II regions: ionization of a central void

To demonstrate the ability of our scheme to handle more complicated situations, we also set up a model with ionization photons. The void region is surrounded by two nested cubes with opposite faces open. The walls of the cubes are set to be  $10^{12}$  denser than the rest of the medium, and the ionizing UV flux is introduced at all faces of the computational volume.

Similar to the test problem of Section 4.2, if  $\beta = 0$ , then the medium will be ionized completely, since there is a constant flux of primordial ionizing photons. The speed of ionization depends on the values of  $\beta$ ,  $\beta$ ,  $g_{\text{HI}}$  and  $n_{\text{H}}$ . Note, however, that if  $\beta$  is too high, the I-front will be very slow, since a large portion of the original ionizing photons are scattered back. On the other hand, if  $\beta$  is too low, the I-front will propagate much faster in those regions where ionization is driven by primordial photons, but in shadowed regions there will be too few recombination photons. Thus, it seems that the speed of ionization of the central void will be

the highest at some intermediate  $\beta$ . In Fig. 4.4 we demonstrate ionization of the void region for models with complete scattering and with no scattering at all.

As expected, for the no-scattering model ( $q = 0$ ) the central region remains neutral, since there is no direct path for the ionizing photons. However, for the model which includes scattering ( $q = 1$ ), the central region eventually becomes ionized. This demonstrates that our scheme is able to deal with re-scattering of the ionizing photons. Beyond this simple test case, there are many astrophysical situations where progress can be made with our method. For example, analytic solutions are often used, which are steady-state, and which assume a sharp boundary between the neutral and ionized zones. Using our numerical techniques it should be possible to follow general systems with complex density inhomogeneities and regions of partial ionization.

## 5 CONCLUSIONS

Ultimately, the choice of numerical technique in radiative transport depends on the type of problem one is trying to solve. The starting point in our discussion is that the photoionization time-scale in the low optical depth regime ( $\tau \ll 1$ ) is of order  $t_{\text{tr}}$ , suggesting that explicit advection might be a faster method in covering at least these regions. We have demonstrated that numerical solution on a time-scale  $t_{\text{tr}}$ , in three dimensions, is possible with existing desk-

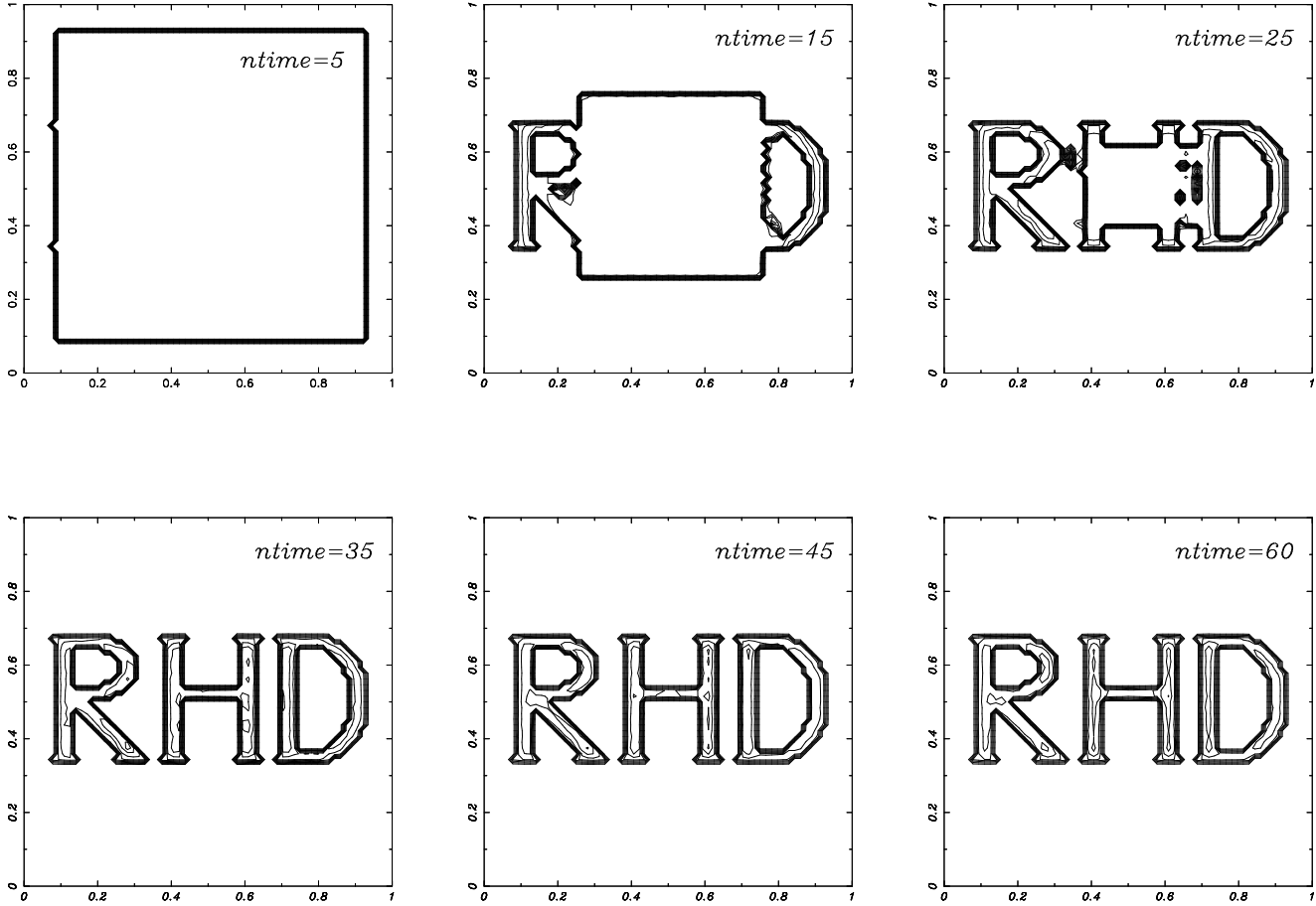


Figure 4. Contour plot of ionization in a cross-section through the data presented in Fig. 4.2. There are 11 contour lines spaced linearly from  $x = 0$  to  $x = 1$ . Note the sharpness of the ionization boundaries.

top hardware. Compared to the elliptic-type solvers on the mid- to time-scale or the time-scale of atomic processes, explicit radiative advection produces very accurate results without the need to solve a large system of coupled non-linear elliptic equations. The computing requirements with explicit advection grow linearly with the inclusion of new atomic and molecular rate equations, which is certainly not the case for quasi-static solvers. Although it is feasible that the development of multigrid techniques for elliptic equations might actually approach similar scaling.

Using equation (1) we can see that the entire history of reionization can be modeled with  $10^4$ – $10^5$  time-steps (depending on the required resolution), which makes explicit advection an attractive choice for these calculations. However, the efficiency of the explicit radiative solver has still to be explored. Future work should include a detailed comparison between explicit advection and implicit reconstruction (through an elliptic solver), to demonstrate which method works best for calculating inhomogeneous reionization.

As we have demonstrated here, for certain problems, including the propagation of supersonic I-fronts, the Courant condition does not seem to impose prohibitively small time steps. In this case the biggest challenge is to accurately describe anisotropies in the radiation field, i.e. to solve for

inhomogeneous advection in the 5D phase space, in the presence of non-uniform sources and sinks of radiation. Strictly speaking, the storage of one variable at, say,  $64^5$  data points requires about 9 GB of memory, which stretches the capabilities of top-end desktop workstations. One attractive possibility for future exploration is to directly solve the monochromatic photon Boltzmann equation in 5D. To demonstrate the feasibility of the numerical solution, however, among different methods, we here chose to concentrate on simple ray tracing at the speed of light. The numerical approach we have used is completely conservative and produces very little numerical dissipation.

The global exchange of energy via the radiation field at a fixed wavelength is probably one of the easiest problems to solve in numerical RT. It seems likely that in the cosmological context, a few years from now, with progress in computer technology, this problem will be routinely solved in three spatial dimensions with the sort of resolution obtained in modern, state-of-the-art hydrodynamical simulations ( $10^7$ – $10^9$  three-dimensional data points).

On the other hand, the full solution of the RHD equations, retaining all  $O(v=c)$  terms, is a much more complicated problem. In this case one deals with frequency-dependent RT, and issues such as line transfer, broaden-



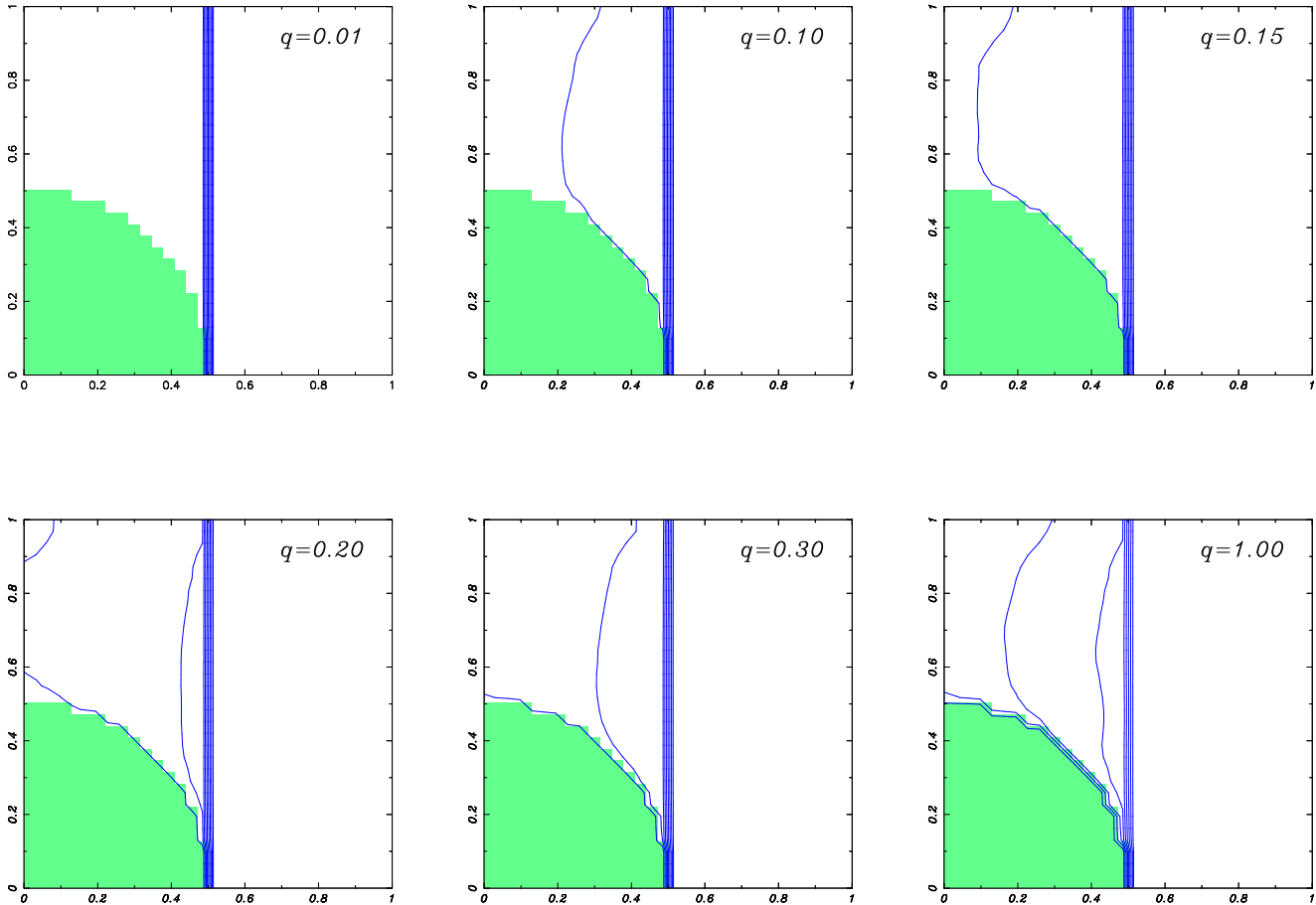


Figure 5. Cross-sections of the dense clump (shaded) and the neutral shadow region behind it, for different fractions  $q = \tau_{\text{rec}}/\tau_{\text{ion}} = \tau_{\text{rec}}/\tau_{\text{ion}}$  of recombination into ground states. The clump is being illuminated with a flux  $F_{\text{ion}}$  of direct stellar ionizing photons coming from below, and the shadow region behind it is being photoionized by recombination Ly $\alpha$  continuum photons from the surrounding H II gas. Each model has been evolved to an equilibrium state, corresponding to many passages of the wavefront across the computational region. The nine contour levels correspond to ionization fractions of  $x = 0.1; 0.2; \dots; 0.9$ , with  $x = 0.1$  being the leftmost line in each panel. This test is adapted from Canto et al. (1998).

ing effects and spatial motions within the simulation box become important. Nevertheless, we want to conclude that with a reasonable expenditure of computational resources, of the type available today, it is possible to numerically model many different aspects of the full 3D radiative transfer problem. And we feel that the methods described here represent a significant and realizable step towards the goal of full cosmological RHD.

#### ACKNOWLEDGMENTS

We wish to thank Taishi Nakamoto for providing us with the results of reionization models from the University of Tsukuba ahead of publication. A.R. would like to thank Jason R. Aman for numerous enlightening discussions, Gregory G. Fabian for constant encouragement on this project, as well as Randall J. LeVeque for help with numerical methods for multidimensional conservation laws. This work was supported by the Natural Sciences and Engineering Research Council of Canada.

#### REFERENCES

- Abel T., Anninos P., Zhang Y., Norman M. L., 1997, *New Astronomy*, 2, 181
- Anninos P., Zhang Y., Abel T., Norman M. L., 1997, *New Astronomy*, 2, 209
- Auer L.H., Mihalas D., 1970, *MNRAS*, 149, 65
- Canto J., Steen W., Shapiro P.R., 1998, *ApJ*, 502, 695
- Couchman H.M.P., Rees M.J., 1986, *MNRAS*, 221, 53
- Evans F., 1998, *J. Atmospheric Sciences*, 55, 429
- Gnedin N.Y., Ostriker J.P., 1997, *ApJ*, 486, 581
- Haiman Z., Loeb A., 1997, *ApJ*, 483, 21
- Haiman Z., Loeb A., preprint astro-ph/9710208
- Kepner J.V., Babula A., Spergel D.N., 1997, *ApJ*, 487, 61
- Madau P., Meiksin A., Rees M.J., 1997, *ApJ*, 475, 429
- Madau P., 1998, preprint astro-ph/9807200
- Meiksin A., 1994, *ApJ*, 431, 109
- Mihalas D., Mihalas B., 1984, *Foundations of Radiation Hydrodynamics*. Oxford University Press, New York
- Navarro J.F., Steinmetz M., 1997, *ApJ*, 478, 13
- Norman M. L., Paschos P., Abel T., 1998, preprint astro-ph/9807282
- Park Y.-S., Hong S.S., 1998, *ApJ*, 494, 605
- Shapiro P.R., 1986, *PA SP*, 98, 1014

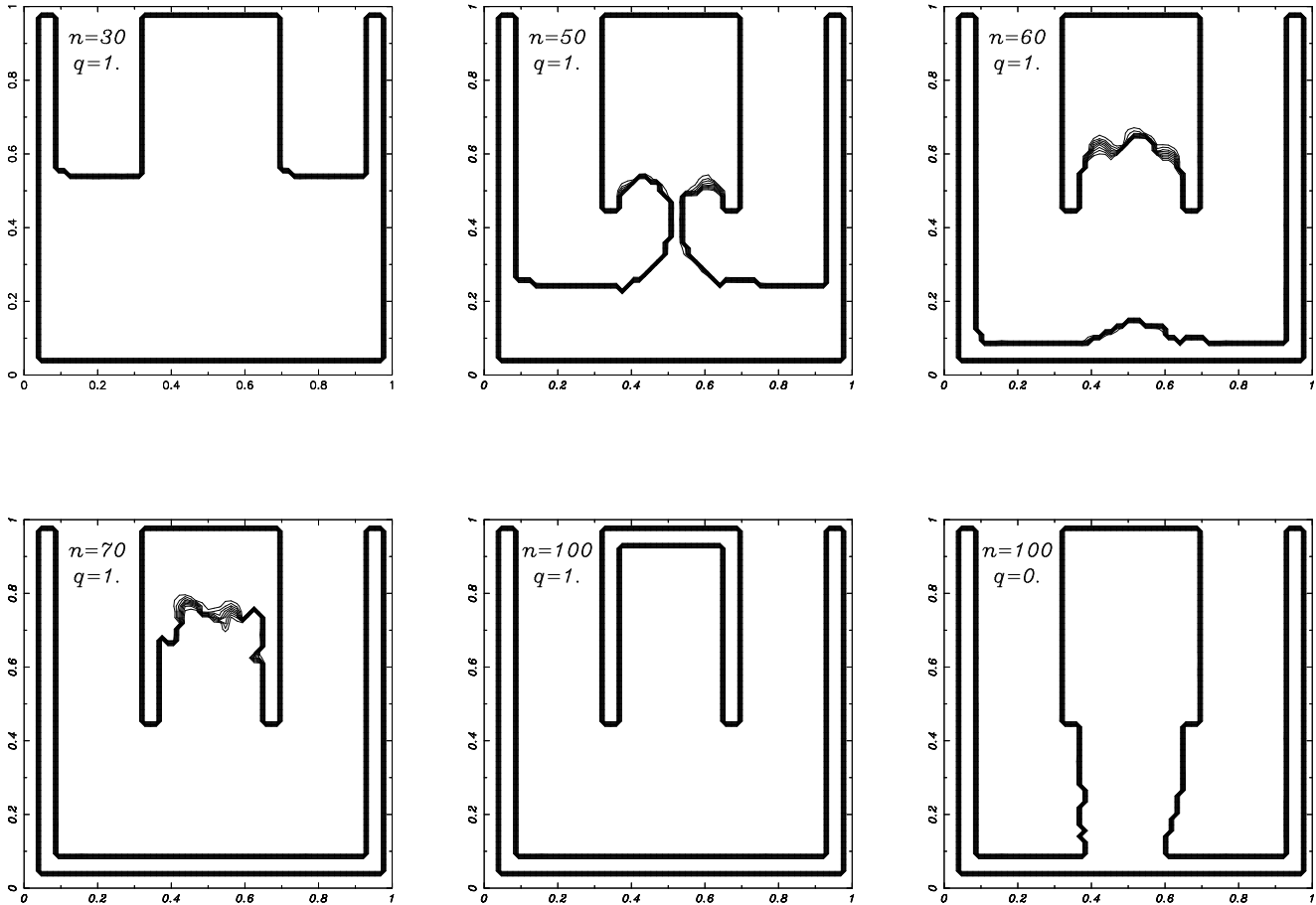


Figure 7. Diagram demonstrating ionization of the void region, which consists of two nested cubes with opposite sides open. The central void and the side ‘tunnels’ have the same density as the surrounding medium, and the density of the walls is set to be  $10^{12}$  higher than that. In this figure we plot one of the central cross-sections showing contours of ionization at various different output times for the model with complete scattering ( $q = 1$ ), and a quasi-equilibrium configuration for the model with no scattering ( $q = 0$ ) after  $n = 100$  time steps.

Shapiro P.R., Raga A.C., Mellem G., 1998, preprint astro-ph/9804117

Spitzer L., Jr., 1968, *Diffuse Matter in Space*. Interscience publishers, New York

Stone J.M., Mihalas D., 1992, *J. Comput. Phys.*, 100, 402

Stone J.M., Mihalas D., Norman M.L., 1992, *ApJS* 80, 819

Tajiri Y., Umemura M., 1998, preprint astro-ph/9806046

Umemura M., Nakamoto T., Susa H., 1998, in Miyama S.M., Shibata K., eds, *Numerical Astrophysics 1998*. Kluwer, in press

Zhang, Y., Meiksin, A., Anninos, P., Norman, M.L., 1998, *ApJ*, 495, 63

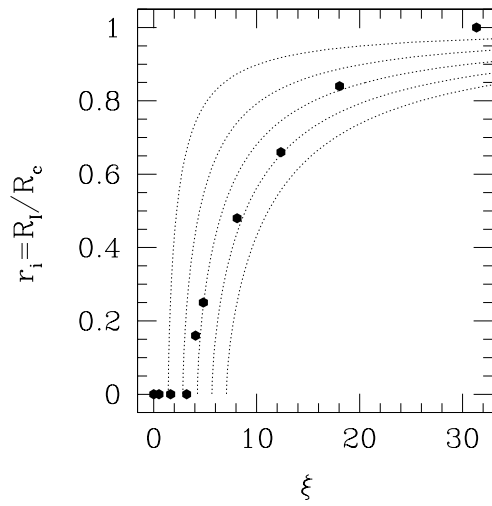


Figure 6. The width  $R_I$  of the shadow behind a neutral clump of radius  $R_c$  as a function of the dimensionless parameter  $\xi$  of Eq. (17). The dotted lines represent the two-stream approximate solution (Canto et al. 1998) for different fluxes of the secondary photons, but assuming an infinitely sharp boundary. The points show the results of our 3D numerical model, plotted explicitly at  $x = 0.1$ . Since the analytic solution is only appropriate for a very idealized system, we would not expect a detailed match with our numerical results; the qualitative shape agrees fairly well.